MNRAS **000**, 1–10 (2019) Preprint 4 November 2019 Compiled using MNRAS LATEX style file v3.0

K2-HERMES II. Complete results C1-C13

Robert A. Wittenmyer,[1]★ Jake T. Clark,[1] Sanjib Sharma,[2] Dennis Stello,[3] Jonathan Horner,[1] Stephen R. Kane,[4] Catherine P. Stevens,[5] Duncan J. Wright,[1] Sarah L. Martell,[3,6] Galah Team[7]

[1] *University of Southern Queensland, Centre for Astrophysics, USQ Toowoomba, QLD 4350 Australia*
[2] *Sydney Institute for Astronomy, School of Physics, University of Sydney, NSW 2006, Australia*
[3] *School of Physics, University of New South Wales, Sydney 2052, Australia*
[4] *Department of Earth and Planetary Sciences, University of California, Riverside, CA 92521, USA*
[5] *Department of Physics, Westminster College, New Wilmington, PA 16172, USA*
[6] *Centre of Excellence for All-Sky Astrophysics in Three Dimensions (ASTRO 3D), Australia*
[7] *School of Hard Knocks*

Accepted XXX. Received YYY; in original form ZZZ

ABSTRACT

Accurate and precise radius estimates of transiting exoplanets are critical for understanding their compositions and formation mechanisms. To know the planet, we must know the host star in as much detail as possible. We present complete results from the K2-HERMES survey, which uses the HERMES multi-object spectrograph on the Anglo-Australian Telescope to obtain R~28,000 spectra for more than 30,000 K2 stars. We present complete host-star parameters, masses, and radii for 178 K2 candidate planets from C1-C13. Our results cast doubt on 18 K2 candidates, as we derive unphysically large radii, larger than $2R_{\rm Jup}$. We discuss the properties of the K2 planet sample as functions of age, metallicity, and other key stellar properties. Our results highlight the importance of obtaining accurate, precise, and self-consistent stellar parameters for ongoing large planet search programs - something that will only become more important in the coming years, as TESS begins to deliver its own harvest of exoplanets.

Key words: stars: fundamental parameters — planets and satellites: fundamental parameters — techniques: spectroscopic

1 INTRODUCTION

With the discovery of the first planets orbiting other stars (Campbell et al. 1988; Latham et al. 1989; Wolszczan & Frail 1992; Mayor & Queloz 1995), humanity entered the 'Exoplanet Era'. For the first time, we had confirmation that the Solar system was not unique, and began to realise that planets are ubiquitous in the cosmos (e.g. Fressin et al. 2013; Winn, & Fabrycky 2015; Hardegree-Ullman et al. 2019). At the same time, we learned that planetary systems are far more diverse than we had previously imagined. We discovered planets denser than lead and more insubstantial than candy floss (Burgasser et al. 2010; Masuda 2014; Marcy et al. 2014; Johns et al. 2018), found myriad systems containing giant planets orbiting perilously close to their host stars (e.g. Mayor & Queloz 1995; Masset & Papaloizou 2003; Bouchy et al. 2005; Hellier et al. 2011; Wright et al. 2012; Albrecht et al. 2012), and discovered others with planets moving on highly elongated, eccentric orbits, similar to those of comets in the Solar system (e.g. Wittenmyer et al. 2007; Tamuz et al. 2008; Harakawa et al. 2015; Wittenmyer et al. 2017). We even uncovered two types of planet that have no direct analogue in the Solar system – the super-Earths and sub-Neptunes (e.g. Charbonneau et al. 2009; Vogt et al. 2010; Winn et al. 2011; Howard et al. 2012; Sinukoff et al. 2016).

The rate at which we found new exoplanets was boosted dramatically by the launch of the *Kepler* spacecraft in 2009. In the years that followed, *Kepler* performed the first great census of the Exoplanet Era. In doing so, it revolutionised exoplanetary science, discovering some 2345 validated planets[1], and finding hundreds of multiply-transiting systems (e.g. Borucki et al. 2010; Batalha et al. 2013; Mullally et al. 2015). After the failure of its second reaction wheel in 2013,

★ E-mail: rob.w@usq.edu.au (RW)

[1] as of 25th October, 2019, from the NASA Exoplanet Archive, https://exoplanetarchive.ipac.caltech.edu/. A further 2420 candidate planets were found during the *Kepler* main mission, and still await confirmation.

the spacecraft was repurposed to carry out the "K2" mission (Howell et al. 2014). *Kepler's* golden years were spent in ~80-day observations of fields along the ecliptic plane, with targets selected by the broader astronomical community for a wide range of astrophysical studies beyond planet search. A total of 20 pointings ("campaigns") were performed until the spacecraft station-keeping fuel was exhausted in 2018 October. Altogether, the K2 mission observed more than 150,000 stars across 20 campaigns, resulting in 392 confirmed and 892 candidate planets to date[2].

With the exception of the small number of directly imaged exoplanets (e.g. Kalas et al. 2008; Marois et al. 2008, 2010; Lagrange et al. 2009), our knowledge of the new worlds we discover has been gleaned indirectly. We observe a star doing something unexpected, and infer the presence of a planet. Our knowledge of the planets we find in this manner is directly coupled to our understanding of their host stars. For example, consider the case of a planet discovered using the transit technique. By measuring the degree to which the light of the planet's host star is attenuated during the transit, it is possible to infer the planet's size. The larger the planet, the more light it will block, and the greater the dimming of its host star. As a result, it is relatively straightforward to determine the size of the planet *relative to its host star*. When converting those measurements to a true diameter for the newly discovered world, however, one must base that diameter on the calculated/assumed size of the host star. Any uncertainty in the size of the host carries through to the determination of the size of the planet.

For that reason, it is critically important for us to be able to accurately characterise the stars that host planets. The more information we have about those stars, and the more precise those data, the more accurately we can determine the nature of their orbiting planets.

Over the past few years, the Galactic Archaeology with HERMES survey (GALAH) has been gathering highly detailed spectra of a vast number of stars in the local Solar neighbourhood (e.g. De Silva et al. 2015; Martell et al. 2017; Buder et al. 2018). The survey uses the High Efficiency and Resolution Multi-Element Spectrograph (HERMES) on the Anglo-Australian Telescope (Freeman 2012; Simpson et al. 2016) to simultaneously obtain spectra for approximately four hundred stars in a given exposure. Analysis of those high-resolution spectra allows the determination of a variety of the properties of those stars, along with the calculation of accurate abundances for up to thirty different elements in their outer atmospheres. GALAH aims to survey a million stars, facilitating an in-depth study of our Galaxy's star formation history - and has already yielded impressive results (e.g. Quillen et al. 2018; Duong et al. 2018; Kos et al. 2018a,b; Zwitter et al. 2018; Gao et al. 2018; Čotar et al. 2019a,b; Žerjal et al. 2019). Whilst the data obtained by the GALAH survey is clearly of great interest to stellar and Galactic astronomers, it can also provide information of critical importance to the exoplanet community. For that reason, in this work we describe the results of the K2-HERMES survey, whose design follows that of the main GALAH program, but is designed specifically to maximise the scientific value of the plethora of exoplanets discovered during *Kepler's* K2 mission.

K2-HERMES is a survey born out of the urgent need for accurate, precise, and self-consistent physical parameters for stars hosting candidate planets. Using the same instrumental setup and data processing pipelines as GALAH, the K2-HERMES survey aims to collect a spectrum for as many K2 target stars as possible. For each target so observed, we compute spectroscopic stellar parameters (T_{eff}, log g, [Fe/H]), as well as the derived physical parameters such as mass, radius, luminosity, and age. The HERMES instrument was specifically designed to measure the chemical abundances of up to 30 elements for the GALAH survey, and so those abundances are also delivered by the standard GALAH data processing pipeline. A forthcoming paper, Clark et al. (2019, in prep), will present a detailed analysis of the chemical abundance results in the context of the *Transiting Exoplanet Survey Satellite* mission, *TESS*.

In this paper, we present the complete results from the K2-HERMES survey for K2 campaigns 1-13. In Section 2, we briefly describe the observing strategy and data analysis procedures, and we detail how the stellar physical parameters have been derived. Section 3 gives the physical properties of the K2 planet candidates and their host stars. Finally, in Section 4, we place our results in context and present our conclusions.

2 OBSERVATIONS AND DATA ANALYSIS

The observational data used here are derived from the K2-HERMES program (Wittenmyer et al. 2018; Sharma et al. 2019), which uses the same instrumental setup as the GALAH survey. We use the High Efficiency and Resolution Multi-Element Spectrograph (HERMES), which can obtain spectra of up to 360 science targets simultaneously (Barden et al. 2010; Brzeski et al. 2011; Heijmans et al. 2012; Sheinis et al. 2015). Target selection for K2-HERMES is essentially unbiased, since the star densities in K2 ecliptic fields are well-matched to the 360 science fibres available for each 1-degree (radius) observing field. [Sarah: I was under the impression that the K2 GAP target selection was highly biased, to focus on RGB stars. What's the difference here?] To prevent excessive cross-talk between fibres, a given field is observed twice, as a "bright" ($10 < V < 13$) and "faint" ($13 < V < 15$) exposure (as described in Martell et al. 2017). Each field contains an average of 210 K2 targets, so the end result is that every K2 target is observed, except those that fall near the corners of the K2 CCD modules (Figure 1). For this study, we selected all K2 planet candidate host stars which had been observed in the K2-HERMES program.

The K2-HERMES survey uses the same instrument as the GALAH survey (Buder et al. 2018), and follows a similar observing strategy. Hence, we use the same reduction pipeline as GALAH to perform the data reduction from the raw CCD images to the final calibrated spectra. The procedure, described fully in Kos et al. (2017) and Sharma et al. (2018), is in brief: (1) raw reduction is performed with a custom IRAF-based pipeline, (2) four basic parameters (T_{eff}, log g, [Fe/H], and radial velocity) and continuum normalisation are calculated with a custom pipeline "GUESS" by

[2] Planet data obtained from the NASA Exoplanet Archive, accessed 25th October, 2019, at https://exoplanetarchive.ipac.caltech.edu/

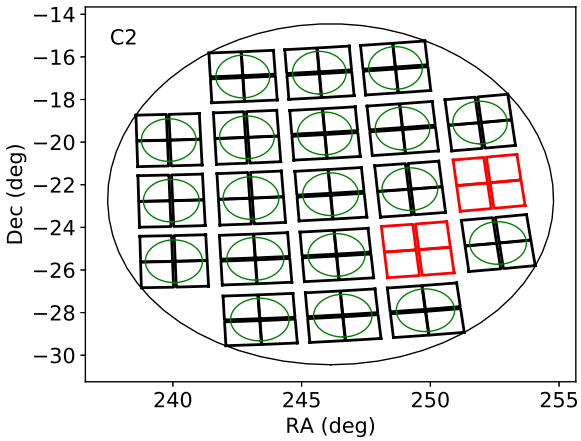

Figure 1. The *Kepler* field of view and the layout of its CCD modules, overlaid with the HERMES field of view (green circles). The red modules are inoperative.

matching the observed normalized spectra to synthetic templates. A grid of AMBRE synthetic spectra is used for this purpose (de Laverny et al. 2012).

2.1 Determination of stellar parameters

The spectroscopic stellar parameters have been estimated with a combination of classical spectrum synthesis for a representative reference set of stars and a data-driven approach to propagate the high-fidelity parameter information with higher precision onto all the stars in the K2-HERMES survey. The method is identical to that used by the TESS-HERMES survey (Sharma et al. 2018), and is briefly outlined as follows. First, we use the spectrum synthesis code Spectroscopy Made Easy (SME) by Piskunov & Valenti (2017) to analyse the reference set. This training set includes samples of stars with external parameter estimates, *Gaia* benchmark FGK stars, and stars with asteroseismic information from K2 Campaign 1 (Stello et al. 2017). Next, we use these SME results as input labels for the training set for *The Cannon* (Ness et al. 2015) to propagate the analysis to all stars. This procedure is identical to that described in the GALAH second data release (Buder et al. 2018).

With a self-consistent set of spectroscopic parameters in hand, we derived the stellar physical parameters using the `isochrones` Python package (Morton 2015). `isochrones` is a Bayesian isochronic modeller that determines the mass, radius and age of stars given various inputs. For our analysis, we utilised the effective temperature (T_eff), surface gravity ($\log g$) and iron to hydrogen abundance ratio ([Fe/H]) along with the available photometric magnitudes **and it tails off here... as if you died while writing it, out of sheer ennui about the delays to this paper**

The resulting stellar parameters are given in Table 1. Our K2-HERMES results have the following median uncertainties: T_{eff}: 72 K, $\log g$: 0.18 dex, [Fe/H]: 0.07 dex, M_*: 0.033 $M_\odot$, R_*: 0.017 $R_\odot$.

Huber et al. (2016) (hereafter H16) presented a catalog of stellar parameters for 138,600 stars in the K2 Ecliptic Plane Input catalog (EPIC) for Campaigns 1-8. Figure 2 shows a comparison of stellar spectroscopic parameters (T_{eff}, $\log g$, [Fe/H]) obtained by K2-HERMES with those given in H16. We find NN matches between the H16 and K2-HERMES catalogs. Only stars hosting confirmed planets are shown here for clarity. **need the numbers here: want median differences between us an H16 for the 3 sets of things**. For T_{eff} and $\log g$, our results are consistent with H16, with a few outliers at T_{eff} ~4000 K, which is expected for the coolest dwarfs in our sample, owing to a paucity of similar stars in the training set (Sharma et al. 2018; Bensby et al. 2014; Torres et al. 2012). In $\log g$, we find 8 stars for which our value is more than 3σ discrepant from H16. Nearly all of these stars were classified by H16 as giants, but we find them to be dwarfs. **14 stars where Teff is 3 sigma out. I'm not sure whether this is a path worth going down?**

Figure 3 shows the comparison between our derived stellar radii and masses and those of H16.

3 PLANET CANDIDATE PARAMETERS

Table 3 gives the properties of the 174 planet candidates from C1-C13 for which the K2-HERMES program has obtained spectra of their host stars. The orbital period and relative radius R_p/R_* are obtained from the NASA Exoplanet Archive, with the relevant references cited in the Table. Where multiple published values exist, the most recent reference was chosen for our analysis. The semimajor axis values have been recalculated based on the orbital period and the revised stellar masses given in Table 1. We derived the planet-candidate radii by multiplying R_p/R_* by the stellar radii obtained by `isochrones` as described above. Uncertainties in the planetary radii result from the propagated uncertainties in R_* and R_p/R_*. As in our previous work (Wittenmyer et al. 2018), for those planet candidates without published uncertainties in R_p/R_*, we adopted the median fractional uncertainty of 0.0025 derived from the catalog of Crossfield et al. (2016).

Using our self-consistent stellar radii, we find the derived planet-candidate radii to lie in a reasonable range for approximately 90% of the planet candidates examined here. We set an upper limit of $2R_{\rm Jup}$ ($22\,R_\oplus$), a radius larger than which no planet has been confirmed. By this criterion, we find 18 candidates with unphysically large radii, and we strongly suspect them to be false positives. All have a disposition status of "candidate" (i.e. not "confirmed") on the NASA Exoplanet Archive, and they are enumerated in Table 4.

We checked the *Gaia* DR2 results for evidence of hidden binarity in these 18 targets. Two stars had highly significant excess astrometric noise (hundreds of sigma): EPIC 202843107 and EPIC 203929178. A further five stars had uncertainties in their absolute radial velocities more then 3σ larger than the expected RV precision for stars of their temperature (Katz et al. 2019). Those are EPIC 201407812, 201516974, 201649426, 201779067, and 212585579. We also flag four stars as giants with $\log g < 3.0$ from our spectroscopic determination. Those giant-star hosts are more likely

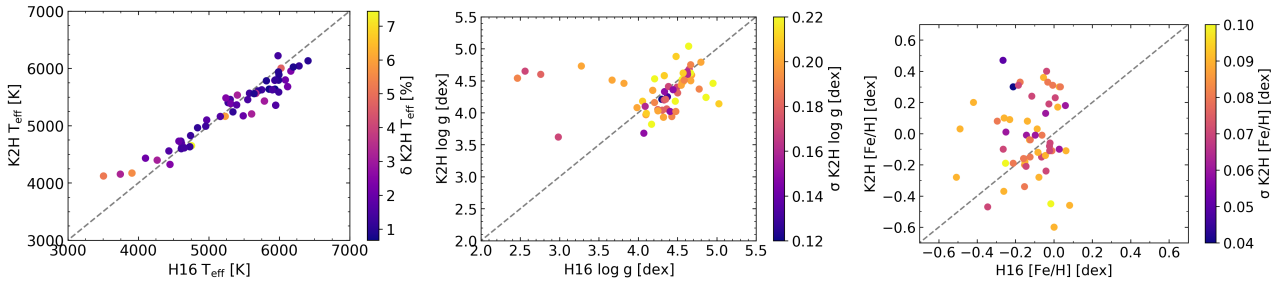

Figure 2. Comparison of our revised spectroscopic stellar parameters with those of H16. The colours of the points represent the uncertainty of the K2-HERMES measurement of that parameter.

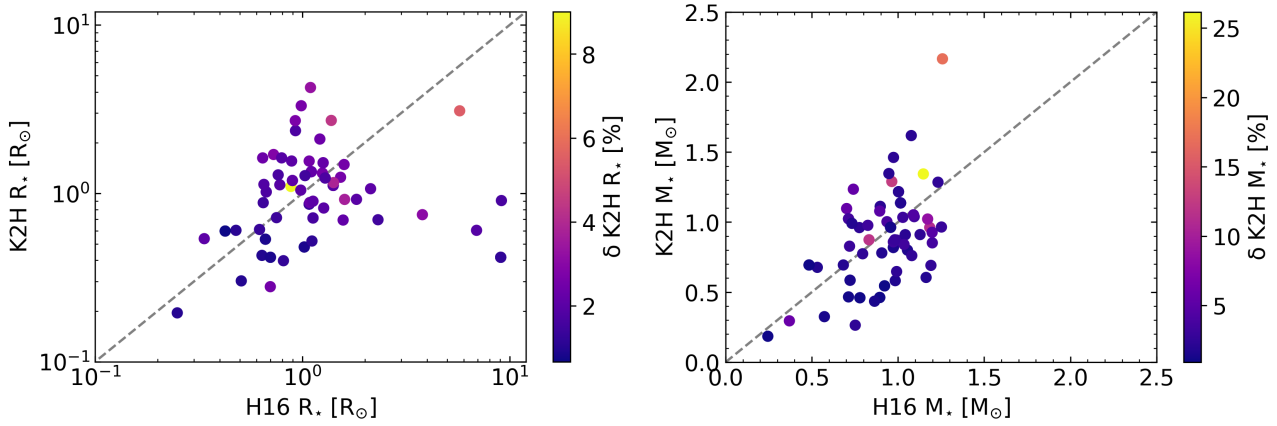

Figure 3. Comparison of our derived stellar physical parameters with those of H16.

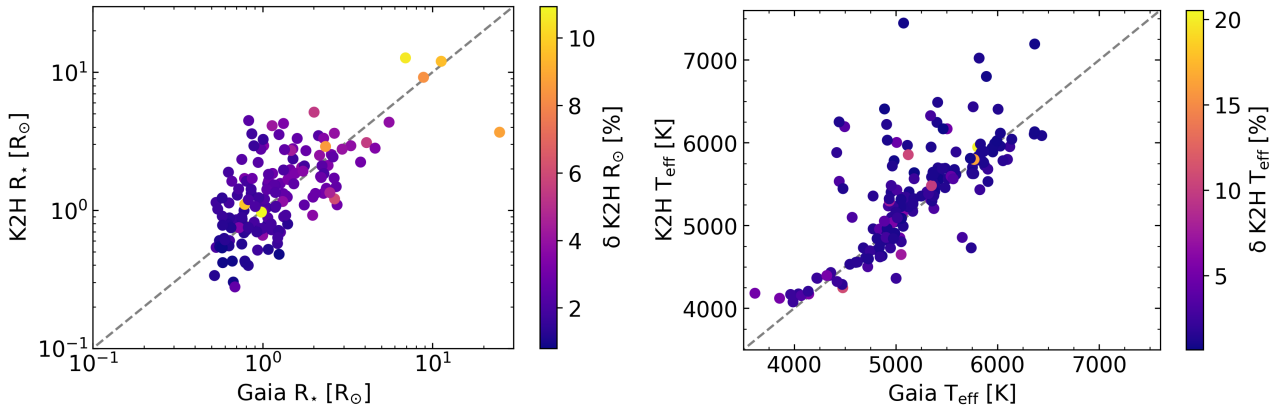

Figure 4. Comparison of our revised stellar radii and T_{eff} with those derived from *Gaia* (Gaia Collaboration et al. 2018).

to be false positives, e.g. wherein a grazing eclipse by an M dwarf can produce the *K*2 transit-like signal, or where the transiting object orbits a different star, as postulated by the analysis of *Kepler* giants in Sliski, & Kipping (2014). Two stars have a weak secondary set of spectral lines, and are marked as binaries here. None of the 18 stars in Table 4 have K2-HERMES-derived stellar parameters that are unusually imprecise, and so we are confident in our disposition of these planetary candidates as false positives due to their unrealistically large inferred radii.

We do find two stars (EPIC 213840781 and 220209578) for which the derived stellar radii are in tension with their log *g*; that is, the surface gravity is that of a dwarf whilst the radius is inflated. **Did something go wrong in isochrones?**

Figure 5 shows the comparison between planet-candidate radii derived in this work and the values from the literature sources (as per the references given in Table 3). The right panel details planets smaller than 4 $R_\oplus$ and differentiates those having previously published radius estimates derived from spectroscopy versus photometry. No systematic trend is evident in our revised planet radii.

A large-scale analysis of spectroscopic parameters for

EPIC	T_{eff}	log g	[Fe/H]	Mass ($M_\odot$)	Radius ($R_\odot$)
201110617	4247.7± 465.7	4.83±0.23	-0.17±0.10	$0.572^{+0.010}_{-0.009}$	$0.552^{+0.006}_{-0.006}$
201127519	4737.0± 58.1	4.23±0.17	0.15±0.07	$0.474^{+0.005}_{-0.006}$	$0.429^{+0.006}_{-0.005}$
201128338	4205.2± 81.0	4.37±0.18	-0.47±0.07	$0.599^{+0.007}_{-0.008}$	$0.546^{+0.005}_{-0.005}$
201132684	5407.0± 54.8	4.37±0.17	0.10±0.07	$0.811^{+0.012}_{-0.012}$	$0.720^{+0.011}_{-0.010}$
201155177	4694.2± 98.1	4.56±0.21	-0.20±0.09	$1.097^{+0.075}_{-0.048}$	$1.623^{+0.038}_{-0.039}$
201264302	4181.5± 207.5	4.33±0.21	-0.48±0.09	$0.418^{+0.003}_{-0.003}$	$0.367^{+0.003}_{-0.003}$
201390927	4288.2± 71.9	4.57±0.19	-0.30±0.08	$0.913^{+0.061}_{-0.054}$	$1.104^{+0.118}_{-0.095}$
201393098	5625.9± 73.6	3.94±0.19	-0.34±0.08	$1.290^{+0.146}_{-0.182}$	$3.313^{+0.089}_{-0.083}$
201403446	6132.3± 59.9	4.05±0.18	-0.47±0.07	$1.039^{+0.037}_{-0.033}$	$1.319^{+0.035}_{-0.033}$
201407812	6404.8± 85.7	4.23±0.17	-0.93±0.07	$1.338^{+0.095}_{-0.108}$	$3.322^{+0.119}_{-0.115}$

Table 1. Spectroscopic and derived stellar parameters. The full version of this table is available online.

EPIC	Incident Flux $F_\oplus$	T_{eq} (K) hot dayside	T_{eq} (K) well-mixed	HZ (au) inner, opt	HZ (au) inner, conserv	HZ (au) outer, conserv	HZ (au) outer opt
201110617.01	446.5	1522.9	1280.6	0.24	0.31	0.57	0.60
201127519.01	31.6	785.4	660.4	0.23	0.29	0.53	0.56
201128338.01	3.0	434.3	365.2	0.23	0.30	0.56	0.59
201132684.01	112.5	1078.9	907.2	0.48	0.61	1.09	1.15
201132684.02	55.2	903.2	759.5	0.48	0.61	1.09	1.15
201155177.01	224.7	1282.6	1078.6	0.85	1.08	1.98	2.09
201264302.01	1369.4	2015.3	1694.7	0.16	0.20	0.37	0.39
201390927.01	282.9	1358.7	1142.5	0.49	0.62	1.16	1.22
201393098.01	249.0	1316.0	1106.6	2.38	3.02	5.35	5.64
201403446.01	110.2	1073.4	902.6	1.09	1.39	2.42	2.55

Table 2. Planetary insolation and habitable-zone boundaries. The full version of this table is available online.

stars hosting *Kepler* planet candidates revealed a "radius gap" (Fulton et al. 2017), with planets of 1.5-2.0$R_\oplus$ apparently depleted by more than a factor of two. Subsequent studies have confirmed that result; Van Eylen et al. (2018) used 117 planets with median radius uncertainties of 3.3% as derived from asteroseismology to further characterise the radius gap. In Figure **??**, we show the distribution of planet-candidate radii from our K2-HERMES sample. **That figure exists but is commented out to keep Overleaf from breaking Jake - wanna say this is a radius gap or a "meh"? Note that I have commented out the radius gap plot since it breaks Overleaf!**.

In Figure 6, we explore the "evaporation valley" in more detail, showing the planet radii as a function of both orbital period and semimajor axis. The radius gap was shown by Van Eylen et al. (2018) to have a slope dependent on orbital period, with a slope of $\frac{\mathrm{dlog}R}{\mathrm{dlog}P}$ of approximately -1/9, a value corroborated by Gupta & Schlichting (2019) and illustrated in Figure 6. In this Figure, we show as filled circles those 95 planets for which we derive radii with precision of 10% or better. The K2 sample investigated here gives consistent results for the shape and slope of this evaporation valley. Figure 7 gives the planet radius as a function of incident stellar flux (Table 2). The hot super-Earth desert postulated by Lundkvist et al. (2016) is shown as a box enclosing the region between 2.2-3.8 $R_\oplus$ and S_{inc} >650 F_{earth}. This region contains only one planet (EPIC 206036749.01) with a radius estimate better than 10% precision. Figure 8 shows the planet radii as a function of host-star mass. We see that smaller planets are markedly less prevalent around higher-mass stars, but this is a wholly-expected consequence: stars more massive than 1 $M_\odot$ in this sample tend to be late F dwarfs or slightly evolved subgiants, which exhibit higher levels of photometric "flicker" (Basri et al. 2013; Bastien et al. 2013, 2014), hindering detection of small planets. The lack of larger planets for stars less than 0.5 $M_\odot$ is also consistent with results from radial velocity surveys of M dwarfs (e.g. Endl et al. 2006; Hatzes 2016; Tuomi et al. 2019).

4 SUMMARY AND CONCLUSION

In this work, we have presented a self-consistent catalog of spectroscopic host-star parameters for 174 *K*2 planet hosts, and the derived physical parameters of 178 planets. We use the revised radii for these planet candidates to cast doubt on 18 as-yet-unconfirmed planets, and we strongly suspect those to be false positives. We also examine the distribution of planet radii as a function of period, showing that the radius gap of the main *Kepler* sample is indeed also evident in this *K*2 sample. The slope of the radius valley is also entirely consistent with that obtained for the *Kepler* planets by Van Eylen et al. (2018) and Gupta & Schlichting (2019).

probably needs some more "wrap up" words here - did we expect trends between planet radius and stellar atmospheric parameters? Is the star mass-planet radius relation (fig. 8) expected? Are there any updated planet radii that are surprisingly small or large?

Our results highlight the importance of accurate stellar parameterisation in the characterisation of newly discov-

EPIC	K2 ID	Reference	P (days)	a (au)	R_p/R_*	R_p ($R_\oplus$)
201110617	K2-156	1	0.813149±0.000050	0.01415±0.00008	0.017041±0.0014	1.03±0.09
201127519		1	6.178369±0.000195	0.05137±0.00020	0.115111±0.0049	5.39±0.24
201128338	K2-152	2	32.6479±0.01483	0.16850±0.00079	0.0344±0.0037	2.05±0.22
201132684.01	K2-158b	2	5.90279±0.00233	0.05960±0.00031	0.0123±0.0012	0.97±0.10
201132684.02	K2-158c	2	10.06049±0.00148	0.08504±0.00043	0.0255±0.0016	2.01±0.13
201155177	K2-42	3	6.68796±0.00093	0.07164±0.00134	0.0304±0.0028	5.39±0.51
201264302		4	0.212194±0.000026	0.00521±0.00001	0.0271±0.004	1.09±0.16
201390927		2	2.638±0.0003	0.03624±0.00076	0.0265±0.0025	3.19±0.46
201393098	K2-7	3	28.6777±0.0086	0.19958±0.00849	0.0177±0.0018	6.40±0.67
201403446	K2-46	1	19.15454±0.002849	0.14188±0.00161	0.01705±0.00127	2.46±0.19
201407812		5	2.8268121	0.04311±0.00110	0.4560	165.41±5.99
201516974		6	36.7099±0.0125	0.19777±0.00479	0.0489±0.0033	23.20±1.80
201546283	K2-27	1	6.771389±0.000062	0.07011±0.00089	0.049112±0.001573	5.89±0.62
201606542		4	0.444372±0.000042	0.01154±0.00014	0.0136±0.002	1.56±0.23
201649426		5	27.770388	0.16878±0.00149	0.3722	31.11±0.47
201754305.02	K2-16b	3	7.61856±0.00096	0.07636±0.00088	0.0268±0.0022	2.98±0.25
201754305.01	K2-16c	3	19.077±0.0033	0.14082±0.00162	0.0299±0.003	3.33±0.34
201779067		5	27.242912	0.20410±0.00539	0.2367	65.47±2.12
201841433		5	12.339133	0.11180±0.00200	0.02881	5.93±0.53
201855371	K2-17	1	17.969079±0.0014	0.11788±0.00071	0.029715±0.003	1.96±0.20
201912552	K2-18	3	32.9418±0.0021	0.11458±0.00044	0.0517±0.0021	1.10±0.05
201923289		5	0.78214992	0.01761±0.00023	0.01346	3.26±0.61
202634963		5	28.707623	0.18192±0.00206	0.2136	29.03±0.90
202675839		1	15.466674±0.0016	0.12123±0.00153	$0.12002^{+0.3}_{-0.062}$	14.31±35.77
202821899		1	4.474513±0.0003	0.05297±0.00096	0.033719±0.0056	4.94±0.85
202843107		5	2.1989041	0.03463±0.00088	0.6032	95.87±20.35
203070421		5	1.7359447	0.03128±0.00040	0.02551	7.71±0.82
203518244		5	0.8411257	0.01921±0.00017	0.01098	2.92±0.67
203533312		4	0.17566±0.000183	0.00626±0.00007	0.0248±0.001	4.63±0.23
203753577		5	3.4007758	0.04250±0.00045	0.06863	7.26±0.95
203771098.02	K2-24b	1	20.885016±0.000438	0.12122±0.00037	0.045111±0.00227	2.36±0.12
203771098.01	K2-24c	1	42.363982±0.000795	0.19425±0.00060	0.061091±0.00174	3.20±0.09
203826436.03	K2-37b	1	4.443774±0.0005	0.04089±0.00015	0.017091±0.01883	0.78±0.86
203826436.01	K2-37c	1	6.429582±0.0003	0.05231±0.00019	0.029105±0.00353	1.33±0.16
203826436.02	K2-37d	1	14.090996±0.001078	0.08825±0.00033	0.027017±0.003572	1.23±0.16
203867512		5	28.465633	0.14947±0.00096	0.1642	9.23±0.22
203929178		3	1.153886±0.000028	0.02131±0.00023	0.53±0.23	167.68±74.42
204221263.02	K2-38b	3	4.01628±0.00044	0.04626±0.00023	0.01329±0.00099	1.04±0.08
204221263.01	K2-38c	3	10.56098±0.00081	0.08813±0.00044	0.0195±0.014	1.52±1.09
204914585		5	18.357773	0.11717±0.00084	0.01924	1.21±0.16
205071984.01	K2-32b	1	8.991942±0.000158	0.08356±0.00036	0.056494±0.0013	5.32±0.14
205071984.03	K2-32c	1	20.661623±0.001762	0.14550±0.00064	0.034033±0.001598	3.21±0.16
205071984.02	K2-32d	1	31.715061±0.002567	0.19361±0.00085	0.037299±0.002528	3.52±0.24
205111664		5	15.937378	0.12421±0.00110	0.02135	2.64±0.32
205570849		3	16.8580±0.0011	0.11461±0.00095	0.047±0.057	3.25±3.94
205924614	K2-55	3	2.849258±00.000033	0.03049±0.00012	0.0552±0.0013	2.58±0.07
205944181		1	2.475641±0.000057	0.03401±0.00011	$0.055833^{+0.19}_{-0.03}$	17.87±60.81
205950854	K2-168	1	15.853989±0.001415	0.11971±0.00095	0.022489±0.001272	2.61±0.16
205957328		1	14.353438±0.001491	0.12268±0.00086	0.023912±0.004385	3.71±0.68
206024342		3	14.637±0.0021	0.10999±0.00076	0.0249±0.0015	2.04±0.13
206026136	K2-57	3	9.0063±0.0013	0.07499±0.00048	0.0308±0.0028	2.05±0.19
206036749		3	1.131316±0.00003	0.02047±0.00013	0.047±0.057	2.73±0.16
206038483	K2-60	3	3.002627±0.000018	0.04118±0.00043	0.06191±0.00035	10.51±0.27
206049452		5	14.454495	0.10956±0.00049	0.02923	2.39±0.21
206055981		5	20.643928	0.13987±0.00093	0.03129	2.66±0.22
206082454.02	K2-172b	1	14.316941±0.001445	0.11953±0.00085	0.017579±0.001495	2.29±0.20
206082454.01	K2-172c	1	29.62682±0.001607	0.19411±0.00137	0.033824±0.001324	4.40±0.20
206096602.01	K2-62b	1	6.671774±0.000177	0.05800±0.00027	0.027246±0.001691	1.59±0.10
206096602.02	K2-62c	1	16.197201±0.00083	0.10477±0.00048	0.026752±0.00269	1.56±0.16
206103150.01	WASP-47b	3	4.159221±0.000015	0.05403±0.00036	0.10214±0.0003	15.00±0.34
206103150.02	WASP-47d	3	9.03164±0.00064	0.09061±0.00061	0.026±0.0015	3.82±0.24
206103150.03	WASP-47e	3	0.789518±0.00006	0.01785±0.00012	0.01344±0.00088	1.97±0.14
206114630		1	7.445026±0.0003	0.07014±0.00065	0.025337±0.033876	2.07±2.77
206125618	K2-64	3	6.53044±0.00067	0.07335±0.00134	0.0259±0.0017	4.81±0.34
206135682		5	5.025831	0.05856±0.00037	0.01961	2.63±0.34
206245553	K2-73	1	7.495692±0.000283	0.06257±0.00034	0.022901±0.001345	1.30±0.08
206417197		4	0.442094±0.000086	0.01129±0.00008	0.0138±0.001	1.34±0.10
210402237	K2-79	1	10.993948±0.000627	0.09243±0.00098	0.027782±0.001543	3.87±0.32
210414957		3	0.969967±0.000012	0.02041±0.00037	0.35±0.15	55.11±23.67
210508766.01	K2-83b	3	2.74697±0.00018	0.03398±0.00012	0.0268±0.0019	1.75±0.12
210508766.02	K2-83c	3	9.99767±0.00081	0.08040±0.00030	0.0319±0.0018	2.08±0.12
210559259		7	14.2683±0.0012	0.10510±0.00116	$0.02854^{+0.0011}_{-0.00082}$	2.21±0.09

EPIC	R_p ($R_\oplus$)	Comments
201407812	165.41±5.99	Double-lined binary. *Gaia* RV error 3.0σ too large
201516974	23.20±1.80	*Gaia* RV error 4.0σ too large
201649426	31.11±0.47	*Gaia* RV error 4.6σ too large
201779067	65.47±2.12	*Gaia* RV error 8.2σ too large
202634963	29.03±0.90	Double-lined binary
202843107	95.87±20.35	*Gaia* astrometric noise 4138σ
203929178	167.68±74.42	*Gaia* astrometric noise 419σ
210414957	55.11±23.67	Large uncertainty from transit depth
211336616	27.06±4.30	log g=2.06±0.18
211390903	25.18±2.33	log g=2.89±0.19
212585579	77.02±70.94	*Gaia* RV error 3.1σ too large
212645891	22.81±18.83	Large uncertainty from transit depth
212688920	36.97±0.80	
213703832	52.47±13.54	log g=2.34±0.21
213840781	130.98±78.19	Large uncertainty from transit depth. **Potentially wonky??**
214741009	576.25±532.27	log g=2.25±0.21
220209578	122.05±105.52	Large uncertainty from transit depth. **Potentially wonky??**
220725183	57.51±2.03	

Table 4. Candidates larger than 22 $R_\oplus$. These candidates are highly likely to be false positives.

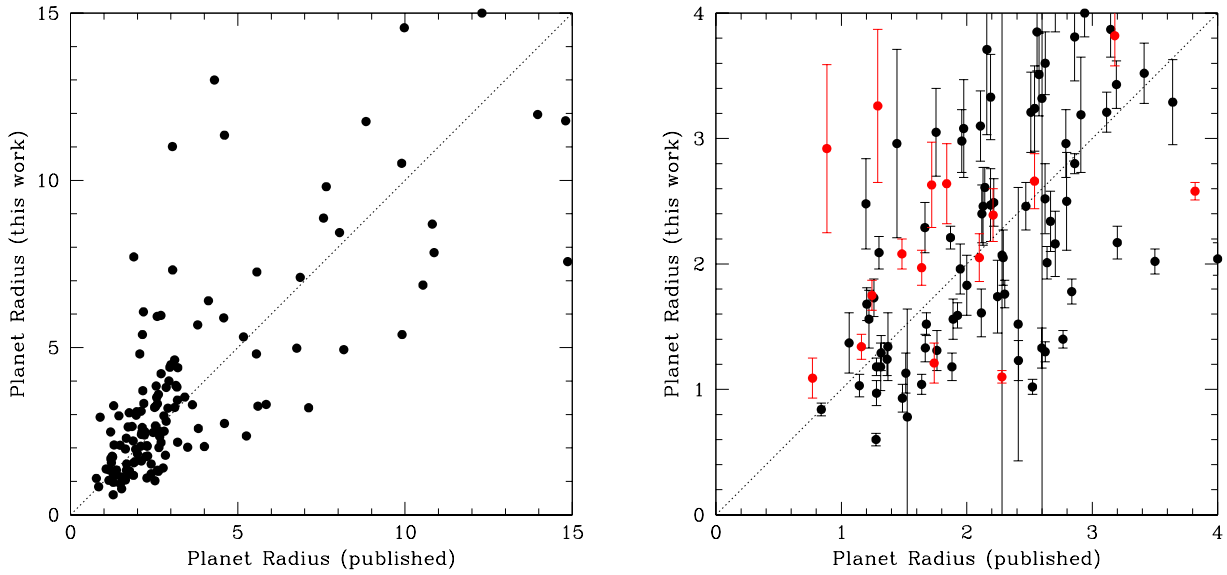

Figure 5. Left panel: Comparison of our derived planetary radii with those from the literature. Error bars have been omitted for clarity. Right panel: Same, but for planet candidates smaller than 4$R_\oplus$. Red points denote published radii derived from photometry, whilst black points are those published values derived from spectroscopy.

ered exoplanets. Fortunately, with surveys like GALAH and instruments like HERMES it is possible to rapidly characterise large numbers of potential exoplanet host stars. In the coming decade, as the exoplanet discovery rate continues to climb, such surveys will prove pivotal in ensuring the fidelity of the exoplanet catalogue. **Should we say something about *Gaia* here, and how that'll help?**

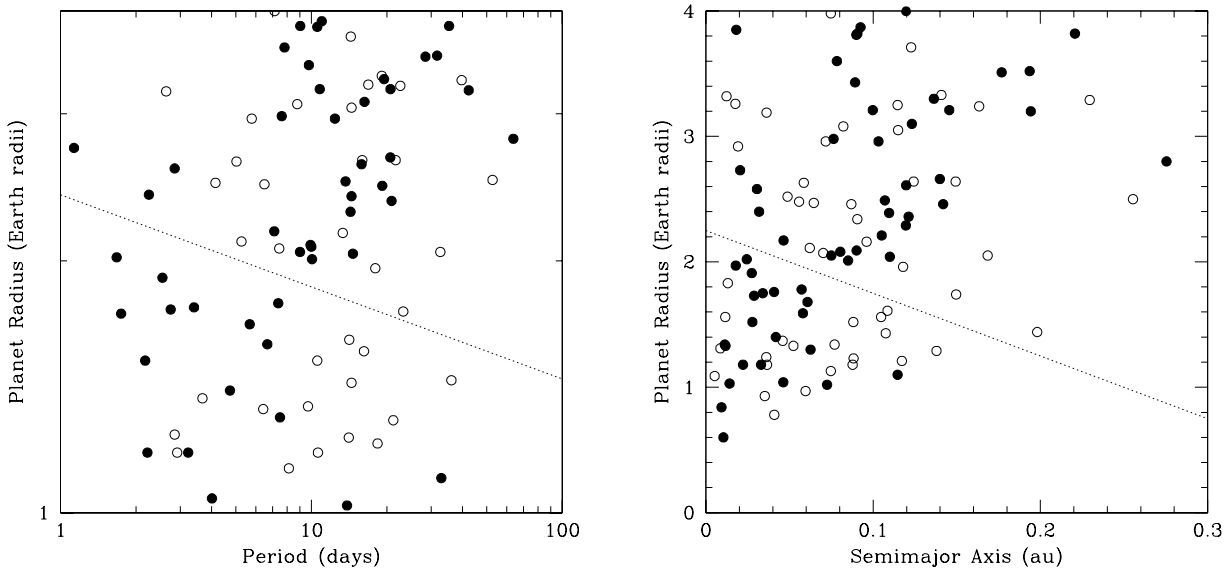

Figure 6. Left: Planet radius versus orbital period; filled circles indicate planets for which we obtain radius estimates at better than 10% precision. The dashed line indicates the slope in the radius valley as noted by Van Eylen et al. (2018) and Gupta & Schlichting (2019). Numbers on the y axis would be helpful Right: Planet radius versus semimajor axis, as computed from the *K*2 period and our derived host-star masses. Symbols have the same meaning as in the left panel.

ACKNOWLEDGEMENTS

D.S. is supported by Australian Research Council Future Fellowship FT1400147. S.S. is funded by University of Sydney Senior Fellowship made possible by the office of the Deputy Vice Chancellor of Research, and partial funding from Bland-HawthornâĂŹs Laureate Fellowship from the Australian Research Council. S.L.M. acknowledges support from the Australian Research Council through Discovery Project grant DP180101791. L.C. is supported by Australian Research Council Future Fellowship FT160100402. This research has made use of NASA's Astrophysics Data System (ADS), and the SIMBAD database, operated at CDS, Strasbourg, France. This research has made use of the NASA Exoplanet Archive, which is operated by the California Institute of Technology, under contract with the National Aeronautics and Space Administration under the Exoplanet Exploration Program. We thank the Australian Time Allocation Committee for their generous allocation of AAT time, which made this work possible. We acknowledge the traditional owners of the land on which the AAT stands, the Gamilaraay people, and pay our respects to elders past, present, and emerging.

REFERENCES

Adams, E. R., Jackson, B., & Endl, M. 2016, AJ, 152, 47
Albrecht, S., Winn, J. N., Johnson, J. A., et al. 2012, ApJ, 757, 18
Barden, S. C., Jones, D. J., Barnes, S. I., et al. 2010, Proc. SPIE, 7735, 773509
Basri, G., Walkowicz, L. M., & Reiners, A. 2013, ApJ, 769, 37
Bastien, F. A., Stassun, K. G., Basri, G., et al. 2013, Nature, 500, 427
Bastien, F. A., Stassun, K. G., Pepper, J., et al. 2014, AJ, 147, 29
Batalha, N. M., Rowe, J. F., Bryson, S. T., et al. 2013, ApJS, 204, 24
Bensby, T., Feltzing, S., & Oey, M. S. 2014, A&A, 562, A71
Borucki, W. J., Koch, D., Basri, G., et al. 2010, Science, 327, 977
Bouchy, F., Udry, S., Mayor, M., et al. 2005, A&A, 444, L15
Brzeski, J., Case, S., & Gers, L. 2011, Proc. SPIE, 8125, 812504
Buder, S., Asplund, M., Duong, L., et al. 2018, MNRAS, 478, 4513
Burgasser, A. J., Simcoe, R. A., Bochanski, J. J., et al. 2010, ApJ, 725, 1405
Campbell, B., Walker, G. A. H., & Yang, S. 1988, ApJ, 331, 902
Charbonneau, D., Berta, Z. K., Irwin, J., et al. 2009, Nature, 462, 891
Čotar, K., Zwitter, T., Kos, J., et al. 2019, MNRAS, 483, 3196
Čotar, K., Zwitter, T., Traven, G., et al. 2019, MNRAS, 1341
Crossfield, I. J. M., Ciardi, D. R., Petigura, E. A., et al. 2016, ApJS, 226, 7
de Laverny, P., Recio-Blanco, A., Worley, C. C., & Plez, B. 2012, A&A, 544, A126
De Silva, G. M., Freeman, K. C., Bland-Hawthorn, J., et al. 2015, MNRAS, 449, 2604

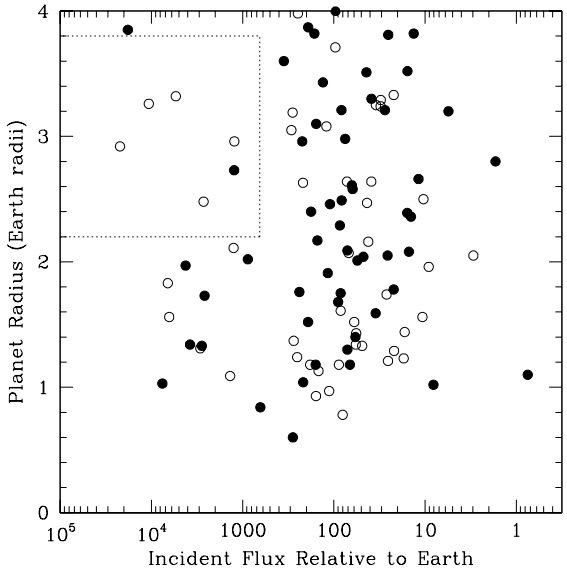

Figure 7. Planet radius versus incident flux, in Earth units. Filled circles indicate planets for which we obtain radius estimates at better than 10% precision. The dashed lines enclose the hot Super-Earth desert (Lundkvist et al. 2016).

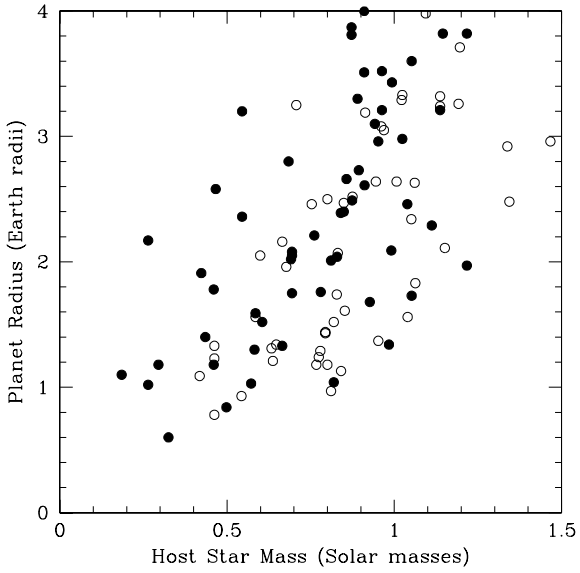

Figure 8. Planet radius versus host-star mass. Filled circles indicate planets for which we obtain radius estimates at better than 10% precision.

Dressing, C. D., Vanderburg, A., Schlieder, J. E., et al. 2017, AJ, 154, 207
Duong, L., Freeman, K. C., Asplund, M., et al. 2018, MNRAS, 476, 5216
Endl, M., Cochran, W. D., Kürster, M., et al. 2006, ApJ, 649, 436
Freeman, K. C. 2012, Galactic Archaeology: Near-field Cosmology and the Formation of the Milky Way, 393
Fressin, F., Torres, G., Charbonneau, D., et al. 2013, ApJ, 766, 81
Fulton, B. J., Petigura, E. A., Howard, A. W., et al. 2017, AJ, 154, 109
Gaia Collaboration, Brown, A. G. A., Vallenari, A., et al. 2018, A&A, 616, A1
Gao, X., Lind, K., Amarsi, A. M., et al. 2018, MNRAS, 481, 2666
Gupta, A., & Schlichting, H. E. 2019, MNRAS, 487, 24
Hardegree-Ullman, K. K., Cushing, M. C., Muirhead, P. S., et al. 2019, AJ, 158, 75
Harakawa, H., Sato, B., Omiya, M., et al. 2015, ApJ, 806, 5
Hatzes, A. P. 2016, Space Sci. Rev., 205, 267
Heijmans, J., Asplund, M., Barden, S., et al. 2012, Proc. SPIE, 8446, 84460W
Hellier, C., Anderson, D. R., Collier-Cameron, A., et al. 2011, ApJ, 730, L31
Howard, A. W., Marcy, G. W., Bryson, S. T., et al. 2012, ApJS, 201, 15
Howell, S. B., Sobeck, C., Haas, M., et al. 2014, PASP, 126, 398
Huber, D., Bryson, S. T., Haas, M. R., et al. 2016, ApJS, 224, 2
Johns, D., Marti, C., Huff, M., et al. 2018, ApJS, 239, 14
Kalas, P., Graham, J. R., Chiang, E., et al. 2008, Science, 322, 1345
Katz, D., Sartoretti, P., Cropper, M., et al. 2019, A&A, 622, A205
Kos, J., Lin, J., Zwitter, T., et al. 2017, MNRAS, 464, 1259
Kos, J., Bland-Hawthorn, J., Freeman, K., et al. 2018, MNRAS, 473, 4612
Kos, J., de Silva, G., Buder, S., et al. 2018, MNRAS, 480, 5242
Lagrange, A.-M., Gratadour, D., Chauvin, G., et al. 2009, A&A, 493, L21
Latham, D. W., Mazeh, T., Stefanik, R. P., Mayor, M., & Burki, G. 1989, Nature, 339, 38
Livingston, J. H., Crossfield, I. J. M., Petigura, E. A., et al. 2018a, AJ, 156, 277
Livingston, J. H., Endl, M., Dai, F., et al. 2018b, AJ, 156, 78
Lundkvist, M. S., Kjeldsen, H., Albrecht, S., et al. 2016, Nature Communications, 7, 11201
Mann, A. W., Gaidos, E., Vanderburg, A., et al. 2017, AJ, 153, 64
Marcy, G. W., Isaacson, H., Howard, A. W., et al. 2014, ApJS, 210, 20
Marois, C., Macintosh, B., Barman, T., et al. 2008, Science, 322, 1348
Marois, C., Zuckerman, B., Konopacky, Q. M., et al. 2010, Nature, 468, 1080
Masset, F. S., & Papaloizou, J. C. B. 2003, ApJ, 588, 494
Martell, S. L., Sharma, S., Buder, S., et al. 2017, MNRAS, 465, 3203
Masuda, K. 2014, ApJ, 783, 53
Mayo, A. W., Vanderburg, A., Latham, D. W., et al. 2018, AJ, 155, 136
Mullally, F., Coughlin, J. L., Thompson, S. E., et al. 2015, ApJS,

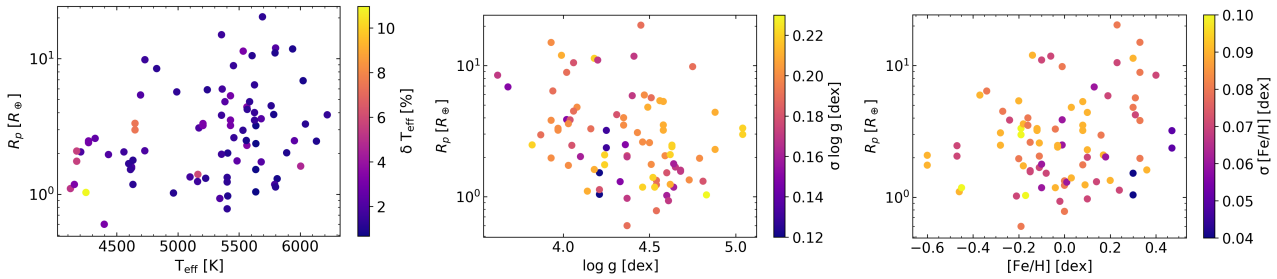

Figure 9. Planet radius versus all the stellar parameters. **Jake: Are these only "CONFIRMED" planets?**

217, 31
Nardiello, D., Libralato, M., Bedin, L. R., et al. 2016, MNRAS, 463, 1831
Ness, M., Hogg, D. W., Rix, H.-W., Ho, A. Y. Q., & Zasowski, G. 2015, ApJ, 808, 16
Mann, A. W., Gaidos, E., Vanderburg, A., et al. 2017, AJ, 153, 64
Martell, S. L., Sharma, S., Buder, S., et al. 2017, MNRAS, 465, 3203
Mayo, A. W., Vanderburg, A., Latham, D. W., et al. 2018, AJ, 155, 136
Mayor, M., & Queloz, D. 1995, Nature, 378, 355
Morton, T. D. 2015, isochrones: Stellar model grid package, ascl:1503.010
Nardiello, D., Libralato, M., Bedin, L. R., et al. 2016, MNRAS, 463, 1831
Petigura, E. A., Sinukoff, E., Lopez, E. D., et al. 2017, AJ, 153, 142
Piskunov, N., & Valenti, J. A. 2017, A&A, 597, A16
Pope, B. J. S., Parviainen, H., & Aigrain, S. 2016, MNRAS, 461, 3399
Quillen, A. C., De Silva, G., Sharma, S., et al. 2018, MNRAS, 478, 228
Schmitt, J. R., Tokovinin, A., Wang, J., et al. 2016, AJ, 151, 159
Sharma, S., Stello, D., Buder, S., et al. 2018, MNRAS, 473, 2004
Sharma, S., Stello, D., Bland-Hawthorn, J., et al. 2019, arXiv:1904.12444
Sheinis, A., Anguiano, B., Asplund, M., et al. 2015, Journal of Astronomical Telescopes, Instruments, and Systems, 1, 035002
Simpson, J. D., De Silva, G. M., Bland-Hawthorn, J., et al. 2016, MNRAS, 459, 1069
Sinukoff, E., Howard, A. W., Petigura, E. A., et al. 2016, ApJ, 827, 78
Sliski, D. H., & Kipping, D. M. 2014, ApJ, 788, 148
Stello, D., Zinn, J., Elsworth, Y., et al. 2017, ApJ, 835, 83
Tamuz, O., Ségransan, D., Udry, S., et al. 2008, A&A, 480, L33
Torres, G., Fischer, D. A., Sozzetti, A., et al. 2012, ApJ, 757, 161
Tuomi, M., Jones, H. R. A., Butler, R. P., et al. 2019, arXiv e-prints, arXiv:1906.04644
Vanderburg, A., Latham, D. W., Buchhave, L. A., et al. 2016, ApJS, 222, 14
Van Eylen, V., Agentoft, C., Lundkvist, M. S., et al. 2018, MNRAS, 479, 4786
Vogt, S. S., Wittenmyer, R. A., Butler, R. P., et al. 2010, ApJ, 708, 1366
Winn, J. N., Matthews, J. M., Dawson, R. I., et al. 2011, ApJ, 737, L18
Winn, J. N., & Fabrycky, D. C. 2015, ARA&A, 53, 409
Wittenmyer, R. A., Endl, M., Cochran, W. D., & Levison, H. F. 2007, AJ, 134, 1276
Wittenmyer, R. A., Jones, M. I., Horner, J., et al. 2017, AJ, 154, 274.
Wittenmyer, R. A., Sharma, S., Stello, D., et al. 2018, AJ, 155, 84
Wright, J. T., Marcy, G. W., Howard, A. W., et al. 2012, ApJ, 753, 160
Wolszczan, A., & Frail, D. A. 1992, Nature, 355, 145
Žerjal, M., Ireland, M. J., Nordlander, T., et al. 2019, MNRAS, 484, 4591
Zink, J. K., Hardegree-Ullman, K. K., Christiansen, J. L., et al. 2019, Research Notes of the American Astronomical Society, 3, 43
Zwitter, T., Kos, J., Chiavassa, A., et al. 2018, MNRAS, 481, 645

APPENDIX A: SOME EXTRA MATERIAL

If you want to present additional material which would interrupt the flow of the main paper, it can be placed in an Appendix which appears after the list of references.

This paper has been typeset from a TEX/LATEX file prepared by the author.